Edited by
Dev Kambhampati

WILEY-VCH

Protein Microarray Technology

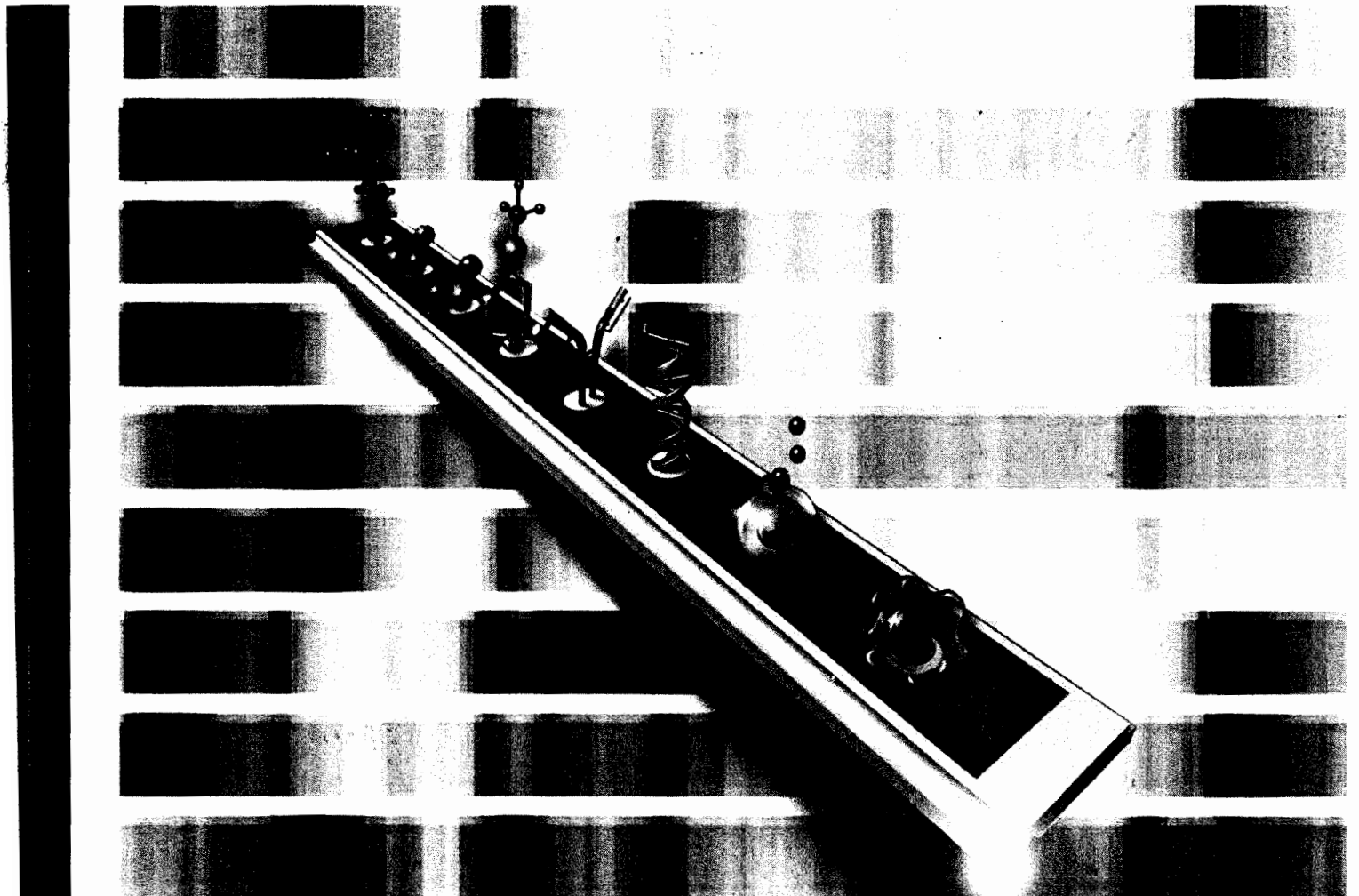

Protein Microarray Technology

Edited by
Dev Kambhampati

WILEY-VCH Verlag GmbH & Co. KGaA

Editor
Dr. Dev Kambhampati
1777 Shoreline Drive, Apt 332A
Alameda, CA 94501
USA

Cover Picture

Library of Congress Card No.: applied for

British Library Cataloguing-in-Publication Data: A catalogue record for this book is available from the British Library.

Bibliographic information published by Die Deutsche Bibliothek
Die Deutsche Bibliothek lists this publication in the Deutsche Nationalbibliografie; detailed bibliographic data is available in the Internet at <http://dnb.ddb.de>

Printed in the Federal Republic of Germany
Printed on acid-free paper

Composition TypoDesign Hecker GmbH, Leimen
Printing Strauss Offsetdruck GmbH, Mörlenbach
Bookbinding Litges & Dopf Buchbinderei GmbH, Heppenheim

ISBN 3-527-30597-1

Contents

Protein Microarray Technology. Edited by Dev Kambhampati

List of Authors

Marko K. Baller
Veeco Instruments, Inc.
112 Robin Hill Road
Santa Barbara, CA 93117
USA

Lisa R. Booth
Prolinx Inc.
22322 20th Avenue SE
Bothell, WA 98021
USA

Julian F. Burke
Genetix Ltd.
Queensway
New Milton, Hamshire BH25 5NN
UK

Robert M. Corn
Department of Chemistry
University of Wisconsin
1101 University Avenue
Madison, WI 53706
USA

Gary Franklin
Biacore AB
Rapsgatan 7
754 50, Uppsala
Sweden

Jürgen Fritz
International University Bremen
School of Engineering and Science
P.O.Box 750 561
28725 Bremen
Germany

Karin A. Hughes, Ph. D.
Senior Product Manager Calbiochem
Biochemicals and Immunochemicals
EMD Biosciences
10394 Pacific Center Court
San Diego, CA 92121
USA

Robert J. Kaiser
Prolinx Inc.
22322 20th Avenue SE
Bothell, WA 98021
USA

Dev Kambhampati
1777 Shorline Drive, Apt 332A
Alameda, CA 94501
USA

Wolfgang Knoll
Max-Planck-Institute for Polymer Research
Ackermannweg 10
55128 Mainz
Germany

Hye Jin Lee
Department of Chemistry
University of Wisconsin
1101 University Avenue
Madison, WI 53706
USA

Stefan Löfås
Biacore AB
Rapsgatan 7
75450 Uppsala
Sweden

LEE O. LOMAS
Ciphergen Biosystems Inc
Fremont CA, 94555
USA

KEVIN P. LUND
Prolinx Inc.
22322 20th Avenue SE
Bothell, WA 98021
USA

CHRISTOPHER J. MANN
Genetix Ltd.
Queensway
New Milton, Hamshire BH25 5NN
UK

ALAN MCWHIRTER
Biacore AB
Rapsgatan 7
754 50, Uppsala
Sweden.

BJÖRN PERSSON
Biacore AB
Rapsgatan 7
75450 Uppsala
Sweden

ANTON PETROV
BioDiscovery Inc.
100 N. Sepulveda Blvd.
Suite 1230
El Segundo, CA 90245
USA

MICHAEL SCHAEFERLING
Institut für Analytische Chemie
Chemo- und Biosensorik
Universität Regensburg
93040 Regensburg
Germany

SOHEIL SHAMS
BioDiscovery Inc.
100 N. Sepulveda Blvd.
Suite 1230
El Segundo, CA 90245
USA

DOUGLAS A. SPICER
Prolinx Inc.
22322 20th Avenue SE
Bothell, WA 98021
USA

SARAH K. STEPHENS
Genetix Ltd.
Queensway
New Milton, Hamshire BH25 5NN
UK

GRETA J. WEGNER
Department of Chemistry
University of Wisconsin
1101 University Avenue
Madison, WI 53706
USA

FANG YU
Max-Planck-Institut
für Polymerforschung
Materialwissenschaften
Ackermannweg 10
55128 Mainz
Germany

5
Surface Plasmon Resonance Imaging Measurements of DNA, RNA, and Protein Interactions to Biomolecular Arrays

GRETA J. WEGNER, HYE JIN LEE AND ROBERT M. CORN

5.1
Introduction

Multi-component arrays of immobilized biomolecules are rapidly becoming essential tools for the screening of bioaffinity interactions. Biomolecular array technology is especially amenable to proteomics research, since much of a protein's function is accomplished through specific interactions with DNA, peptides, and other proteins. Array-based assay formats have been developed both for the detection of proteins in a sample [1], and for the identification of new protein–protein interactions [2,3]. Arrays are also now regularly employed for fundamental studies of protein binding interactions. For example, peptide arrays have been used to study the binding interactions of antibodies [4,5] and to characterize the sequence-specific activity of enzymes [6,7]. Arrays of proteins have also been used for the high-throughput screening of protein–protein interactions and to identify novel biochemical activities [2,3].

The majority of array-based assays currently employ fluorescent, enzymatic or radiolabeled biomolecules. Further advancement of analytical systems that do not require labeled biological molecules to detect affinity binding interactions is needed. Surface plasmon resonance (SPR) imaging is emerging as a label-free surface sensitive optical technique that measures the adsorption of solution phase molecules to arrays of biomolecules on thin gold films by changes in the local index of refraction. Label-free detection is particularly advantageous for the assay of small molecule-binding to proteins, since labels can interfere with the biological activity of the target molecule. To date, SPR imaging has been used to study reversible protein binding to DNA, peptide, protein, and carbohydrate arrays [8–10].

This review summarizes the recent advances that we have made in the implementation of SPR imaging to study DNA, RNA, and protein interactions with DNA, peptide and protein probes immobilized in an array format. After a brief description of the SPR imaging technique in Section 5.2, two surface attachment chemistries used for the covalent immobilization of thiol-modified DNA, peptides, and carbohydrates through the modification of self-assembled monolayers of alkanethiols are discussed in Section 5.3. In Section 5.4, an array fabrication method based on chemical protection and photopatterning is described. Several examples

Protein Microarray Technology. Edited by Dev Kambhampati

ISBN: 3-527-30597-1

of SPR imaging experiments using photopatterned arrays are presented including the study of DNA–DNA hybridization and protein–DNA binding interactions. We will conclude this rchapter in Section 5.5 with a second array fabrication method based on microfluidic stenciling and address its application to peptide–protein and protein–protein binding interactions.

5.2
Surface Plasmon Resonance Imaging

Surface plasmon resonance (SPR) measurements are surface-sensitive optical methods used to characterize organic and biological layers on gold or noble metal thin films. These measurements utilize the optical field enhancement that occurs at a metal/dielectric interface when surface plasmons are created. Surface plasmons are electromagnetic waves, excited by p-polarized light, that propagate parallel to the gold surface. The optical fields decay exponentially from the surface of the metal and have a maximum decay length of about 200 nm. Within this region, the optical fields are sensitive to changes in the index of refraction caused by the adsorption or desorption of molecules onto the surface. As a consequence, SPR experiments have been amenable for the label-free study of reversible biomolecule binding interactions on gold films in real-time using two different methods: (1) scanning angle SPR and (2) SPR imaging techniques.

Angle shift measurements are the most commonly undertaken SPR technique and have been popularized by the commercial Biacore instrument. In a scanning angle experiment, the percentage of light reflected off of a thin gold film optically coupled to a prism is measured as a function of incident angle. A prism or grating coupling arrangement is required because surface plasmons cannot be excited directly at planar air/metal or water/metal interfaces because momentum-matching conditions are not satisfied. A hemispherical prism is used to tightly focus light from a laser onto a single region of a gold thin film. Figure 5.1 shows three SPR curves and their theoretical fits where the percent reflectivity of light is measured as a function of the incident angle for light with excitation wavelengths of 1152 (Δ), 814 (❑), and 633 nm (○) Δ [11]. For the SPR curve measured at an excitation wavelength of 814 nm, increasing the incident angle from 50 to 50.8° causes nearly 100% of the light to be reflected as the critical angle is reached and total internal reflection occurs. Further increase in the angle results in a steep drop in percent reflectivity as light is incorporated into surface plasmons until a minimum is reached at 53.5°, the surface plasmon angle. The position of the SPR angle is sensitive to changes in the index of refraction and/or thickness of the adsorbed film causing the minimum to shift. Shifts in angle position can be correlated to changes in thickness or index of refraction using N-phase Fresnel calculations as described by Hansen [12]. SPR measurements can be enhanced by using near-infrared excitation wavelengths between 800 and 1100 nm. Mid-IR light results in sharper SPR curves than those obtained at an excitation wavelength of 633 nm

from a HeNe source (refer to Figure 5.1). This allows a more precise determination of the SPR angle and can be used to measure thicker films.

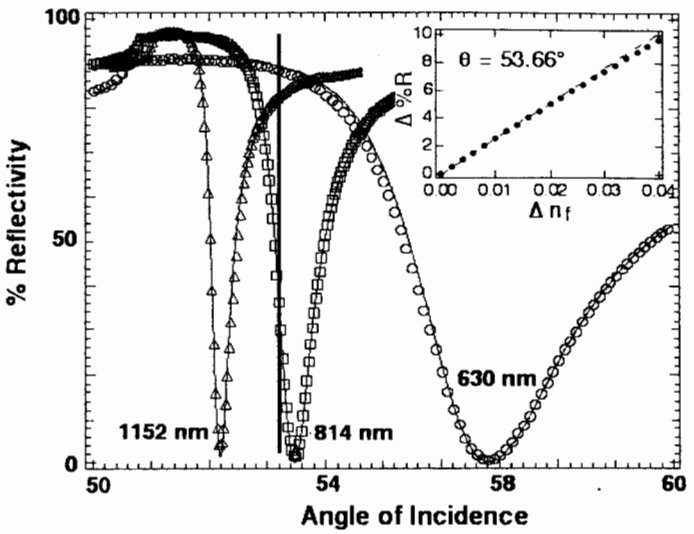

Figure 5.1 SPR reflectivity curves showing the relationship between percentage reflectivity and angle of incidence for excitation wavelengths of 1152 nm (Δ), 814 nm (❑), and 633 nm (○) for an SF-10 glass/Au/water *(in situ)* assembly. Solid lines show the theoretical fit obtained by three-phase Fresnel calculations. Sharper SPR curves are obtained with increasing wavelength and can be applied to study thicker films with angle shift measurements and to enhance the contrast of SPR imaging experiments. The angle at which SPR imaging measurements are obtained is marked by a vertical line on the SPR reflectivity curve obtained at an excitation wavelength of 814 nm. Inset shows the relationship between the change in percentage reflectivity (Δ%R) and the change in index of refraction (Δn_f) at a fixed incident angle of 56.33°. A linear relationship is observed for Δ%R less than 10%. Reprinted with permission from *Analytical Chemistry*, 71 3928–3934, copyright 1999 American Chemical Society and *Analytical Chemistry*, 73 1–7, copyright 2001 American Chemical Society.

While scanning angle experiments are used to study a single region on a gold surface, SPR imaging is used to monitor the spatially resolved adsorption of biomolecules onto a multicomponent array. This technique is especially important for biological experiments where the simultaneous measurement of multiple interactions on a single chip is desired. SPR imaging measurements of the change in percent reflectivity are performed at a fixed angle near the SPR angle, as shown by a vertical line passing through the SPR reflectivity curve measured using an excitation wavelength of 814 nm as shown in Figure 5.1. Figure 5.2 shows a schematic representation of the SPR imaging instrument used to detect the adsorption of biopolymers in solution to surface-immobilized biomolecules such as DNA and peptides [11]. A collimated white light source is coupled with a narrow band pass filter centered at 830 nm and used in place of a laser source. By using this configuration, laser fringes which can interfere with image quality are avoided and the enhanced contrast obtained using an NIR source is maintained. Images with lateral resolutions on the order of 50 μm can be obtained using an excitation wavelength of 830 nm. The light is passed through a polarizer in a direction incident to

a high index glass prism/sample assembly. Here, light impinges on the back of a sample consisting of a gold thin film chemically modified with an array of biomolecules. Analytes are delivered to the array by either a 500-µL flow cell or through a set of parallel microfluidic channels from PDMS requiring 1 µl of sample per channel. Images are collected using a CCD camera after the light reflected off the sample is passed through a narrow band pass filter. The light interacts with the biomolecules immobilized on the thin gold film to create surface plasmons, inducing attenuation in the light reflected from the surface. As biomolecules from solution adsorb onto the array, the local index of refraction changes causing an increase in the percentage of incident light reflected off each array element of the sample, at a fixed optimal angle. The lower left corner of Figure 5.2 contains a typical SPR difference image showing sequence-specific adsorption of complementary DNA onto a two-component DNA array.

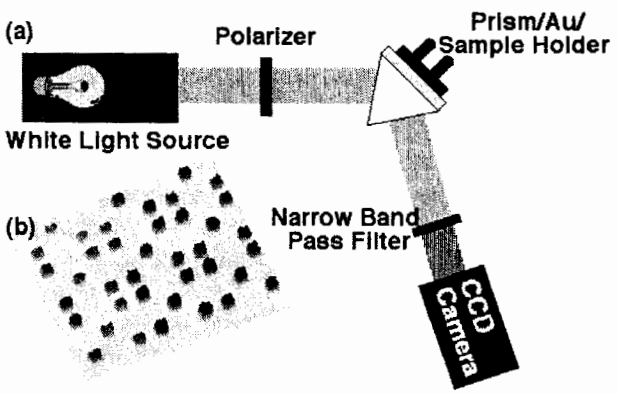

Figure 5.2 Schematic diagram of the surface plasmon imager apparatus. P-polarized white light impinges on a prism sample apparatus at a fixed optimal angle, near the surface plasmon angle. The light is then passed through a narrow band pass filter and images are collected by a CCD camera. The analyte is delivered to the array fabricated on a gold thin film using a simple 500 µL flow cell. An SPR difference image of the sequence-specific hybridization of 18-mer DNA to a two-component DNA array is shown in the bottom left corner of the figure. A maximum of 160 array elements can be studied on one SPR chip with a total surface area of 0.8 cm^2 using square elements with 500 µm widths. (see Colour Plate p. XXIII).

Like the scanning angle SPR measurements, quantitative information can be obtained from SPR imaging measurements. The inset in Figure 5.1 shows the relationship between the percentage reflectivity and the index of refraction for changes in percentage reflectivity under 10% [13]. This relationship can also be applied to determine the surface coverage of biomolecules adsorbed onto a surface. SPR imaging measurements have been used for the quantitative evaluation of the interactions between biomolecules in solution and DNA or peptide probes immobilized on the array. In the case of biomolecules that have a high molecular weight, the number of immobilized surface target sites can be decreased in order to stay within this linear Δ %R region [10]. The sensitivity of the SPR imaging approach is about 10 femtomoles (1 µL of a 10 nM solution) for 18-mer single-stranded DNA

hybridized to a DNA array [14], and 1 femtomole (1 μL of a 1 nM solution) for specific antibody adsorption onto a peptide array [10]. Although SPR imaging measurements do not match the sensitivity of fluorescence or radioactive methods, it is more than adequate for many applications including the study of protein–protein interactions and has the advantage of employing direct detection of binding interactions.

5.3
Surface Attachment Chemistries

The development of well-characterized surface chemistries for the attachment of biological molecules onto gold thin films in an array format is necessary for SPR imaging measurements of biomolecular affinity interactions. Noble metal thin films are required for the propagation of surface plasmons. As a consequence, commercially available DNA arrays made on glass substrates, such as those produced by Affymetrix [15–18], or peptide arrays prepared by the SPOT synthesis technique on cellulose membranes [19–21], are not viable options for SPR imaging investigations. Instead, we have employed self-assembled monolayers of long chain alkanethiols that are ω-terminated with an amine functional group as the foundation of the array [8,9,11,22]. Chemical modification of the self-assembled monolayers is used to tether biological molecules to the surface. In this section, two methods using the bifunctional linkers SSMCC (sulfosuccinimidyl 4-(*N*-maleimidomethyl) cyclohexane-1-carboxylate) and SATP (*N*-Succinimidyl S-acetylthiopropionate) are described for the covalent attachment of thiol-containing DNA, peptide, carbohydrate and capture probe molecules.

5.3.1
SSMCC Attachment Chemistry

In the first reaction scheme, the heterobifunctional linker SSMCC, which contains both an N-hydroxysulfosuccinimide (NHSS) ester and a maleimide functionality, is used to covalently link the amine-terminated self-assembled monolayer of 11-mercapto-undecylamine (MUAM) to a thiol-modified probe molecule (Figure 5.3a) [8,22]. First, the NHSS ester moiety of SSMCC is reacted with the free amines of the alkanethiol monolayer to form amide bonds terminating with maleimide groups. Next, thiol-modified DNA or cysteine-containing peptides are introduced to the thiol-reactive maleimide monolayer and attached by the creation of a thioether bond. DNA molecules attached by this method have a surface coverage of 1.0×10^{12} molecules cm^{-2} [13].

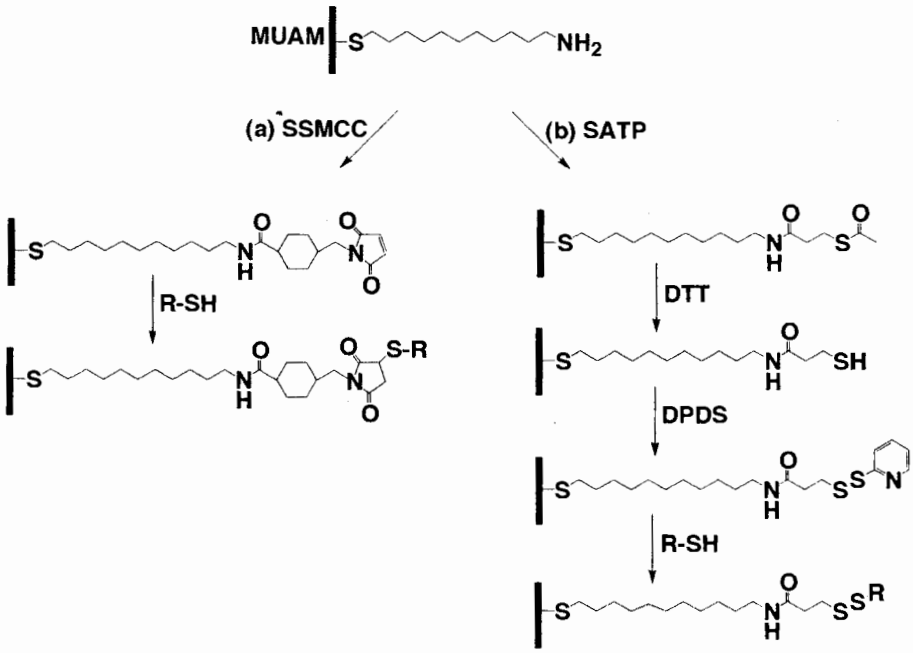

Figure 5.3 Surface attachment chemistry for the immobilization of thiol-modified DNA and cysteine-containing peptides: (a) The linker SSMCC is reacted with a well-packed self-assembled monolayer of 11-mercaptoundecylamine (MUAM) to create a maleimide-modified surface. The maleimide surface is then used to covalently attach thiol-modified DNA or cysteine-containing peptides. (b) In the second approach, SATP is reacted with MUAM to create a protected thiol surface. Upon deprotection with a basic solution containing DTT, the free sulfhydryl is reacted with dipyridyl disulfide to create a pyridyl disulfide surface. Thiol–disulfide exchange reactions are used to couple thiol-containing biomolecules to the surface.

5.3.2
SATP Attachment Chemistry

An alternative reaction scheme, more amenable for generating peptide arrays, involves the attachment of thiol-containing biomolecules onto gold surfaces through a disulfide linkage [10,23]. The reaction scheme for this surface modification process is shown in Figure 5.3b. In this approach, a self-assembled monolayer of MUAM is reacted with the molecule SATP, a bifunctional linker containing an NHS ester and a protected sulfhydryl. The NHS ester reacts with the amines present on the surface to form a stable amide bond resulting in a protected sulfhydryl surface. Exposure of the surface to an alkaline solution containing DTT removes the protecting acetyl group revealing an active sulfhydryl surface. Next, the sulfhydryl surface is reacted with 2,2'–dipyridyl disulfide to form a pyridyl disulfide surface. Thiol-disulfide exchange reactions are then performed in order to attach thiol-modified DNA or cysteine-containing peptides to the substrate, with a surface coverage of 10^{13} molecules cm^{-2}. This type of surface attachment chemistry has the advantage of being reversible, as the disulfide bond can be cleaved in the presence of DTT to regenerate the sulfhydryl-terminated surface.

5.4
SPR Imaging Experiments Using Photopatterned Arrays

Arrays used for SPR imaging experiments contain multiple individually addressable components and are prepared by a combination of self-assembly, surface attachment chemistry, and array patterning using either photopatterning or PDMS microfluidic channels. This section will explore the first array fabrication methodology developed within our laboratories for the creation of robust DNA and peptide arrays using chemical protection and deprotection and photopatterning. This multi-step fabrication procedure is outlined in Figure 5.4 [8]. The first step of the fabrication method is the creation of a temporary hydrophobic background using the bulky amine protecting group, 9-fluorenylmethoxycarbonyl (Fmoc), frequently used in solid phase peptide synthesis. The N-hydroxysuccinimide ester of Fmoc (Fmoc-NHS) is reacted with the terminal amines of a packed-self assembled alkanethiol monolayer to form a stable carbamate linkage. The surface is then exposed to UV light through a patterned quartz mask to create arrays composed of 500 by 500 μm square elements with 500 μm spacing between the elements. The gold–thiol bond is cleaved in the regions where the light shines through the mask resulting in a patterned gold surface that consists of bare gold pads surrounded by Fmoc. Next, the surface is immersed in an ethanolic solution of MUAM. The amine-terminated alkanethiols self-assemble in the bare gold pads producing a surface containing reactive hydrophilic MUAM pads surrounded by the hydrophobic Fmoc background. The lower left-hand corner of Figure 5.4 contains an image of an array showing the individually addressable hydrophilic spots surrounded by a hydrophobic background. Chemical protection allows droplets of hydrophilic DNA or peptides to be "pinned", without contaminating other sequences contained on neighboring pads on the array, and covalently attached using the linkers SSMCC or SATP. These arrays can be easily used with a mechanical array spotter to introduce multiple peptide or DNA elements onto one chip for high-throughput studies. For example, arrays composed of more than 300 elements can be produced using square elements with 250-μm widths.

The array fabrication is then completed by removing the hydrophobic Fmoc background and replacing it with polyethylene glycol (PEG) to reduce the non-specific adsorption of biopolymers. Since Fmoc is a base-labile protecting group, the original amine-terminated surface can be easily regenerated by exposure to a secondary amine. An NHS derivative of polyethylene glycol (PEG) can react with the terminal amines of the SAM to form a stable amide linkage. The formation of the temporary Fmoc surface is necessary, since PEG is too hydrophilic to prevent contamination between DNA or peptide droplets. The DNA arrays can then be analyzed by SPR imaging using a 500 μL flow cell to introduce biopolymer analytes to the array surface. DNA arrays fabricated using SSMCC attachment chemistry can be used for more than 25 hybridization cycles [13] while the SATP chemistry can be used for more than 30 cycles without degradation of the array [23].

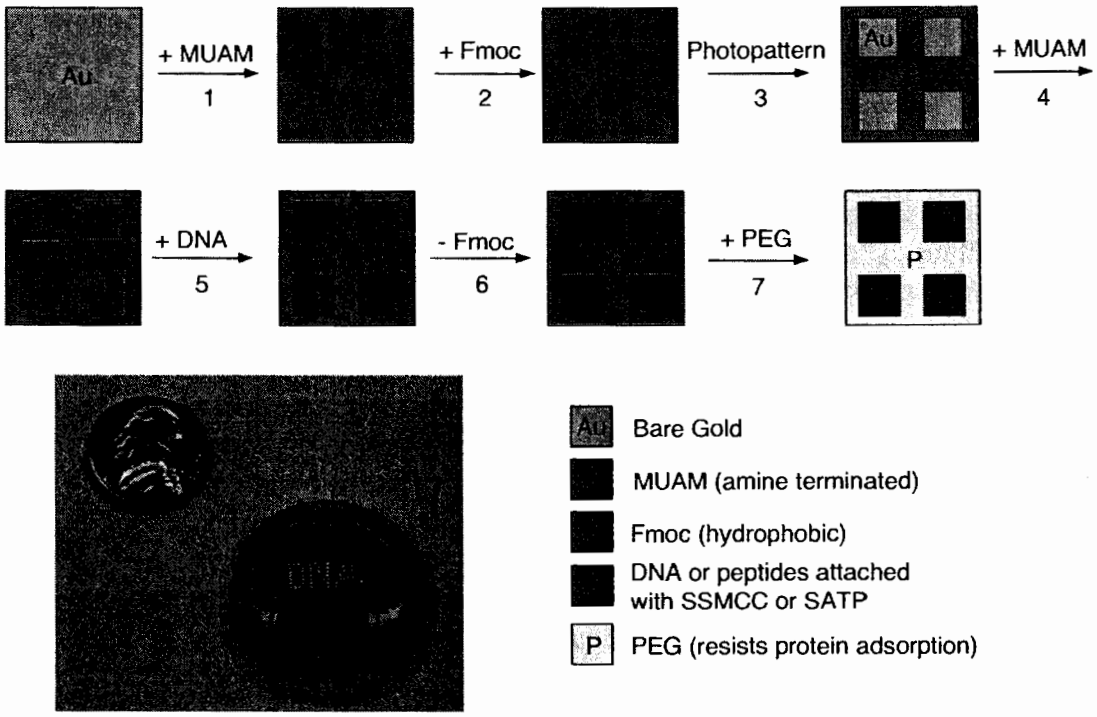

Figure 5.4 Multi-step array fabrication process using protection/deprotection chemistry and photopatterning techniques to prepare DNA and peptide arrays. The bottom left corner of the figure shows individually addressable hydrophilic drops of DNA pinned to the surface by a hydrophobic background. First, a bare gold surface is modified with a self-assembled monolayer of 11-mercapto-undecylamine (MUAM). This amine-terminated surface is reacted with the hydrophobic protecting group Fmoc. UV-light is used to break the gold–thiol bond and create bare gold pads on the surface. These pads are subsequently filled with MUAM. A bifunctional linker is used to attach DNA or peptide probes to create an array. Finally, the Fmoc is removed with base and replaced with a polyethylene derivative to prevent the non-specific adsorption of biopolymers to the background. Reprinted with permission from *Journal of the American Chemical Society*, **121**, 8044–8051. Copyright 1999 American Chemical Society. (see Colour Plate p. XXIV).

5.4.1 DNA–DNA Hybridization

The hybridization of complementary DNA to a five-component DNA array fabricated by photopatterning and SSMCC chemistry was examined by SPR imaging. All surface-immobilized DNA probes were tested by hybridization to respective perfect-match DNA complements. The probes were immobilized in a distinct geometric pattern to easily identify interacting sequences. The DNA sequences used in this experiment are listed in Table 5.1, and denoted as A–E. The surface was first exposed to a 100 nM solution of the 16-mer DNA oligonucleotide complement to probe A for 15 min (Figure 5.5a). The SPR difference image shown in this figure was produced by subtracting the images taken before and after hybridization. Regeneration of the surface was achieved by rinsing with 8 M urea. Repeated cycles of hybridization and denaturation were used to obtain Figure 5b–e. Excellent

sequence-specific adsorption of the complementary DNA was observed for all probes and with little non-specific adsorption to the background. The approximately equal SPR signal under identical experimental conditions indicates that the probes are equally accessible for hybridization to target molecules in solution.

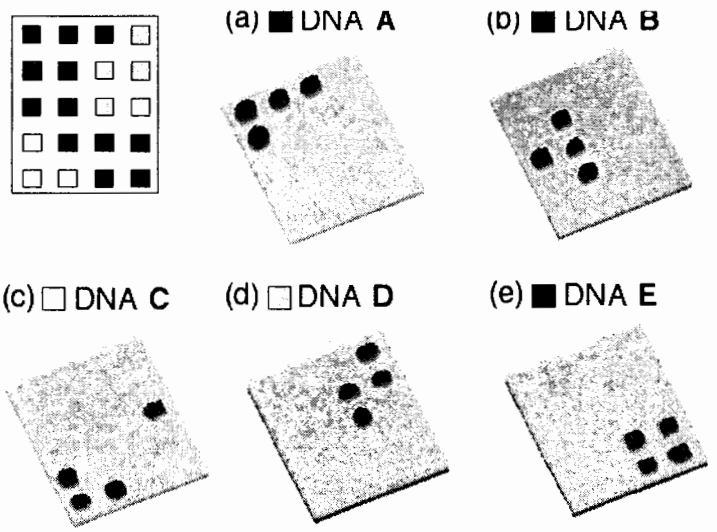

Figure 5.5 SPR difference images showing the hybridization of perfect-match DNA complements to a DNA array containing five different probes. The sequences were immobilized on 500 by 500 μm array elements in the pattern shown in the figure. (a) First, the array was exposed to a 100 nM solution of the DNA complement to probe A for 15 min. Hybridization adsorption onto the array is indicated by a change in the percentage reflectivity of incident light. (b) After rinsing with 8 M urea to regenerate the surface, the experiment was repeated with the DNA complement of probe B. Successive rounds of denaturation and hybridization of the remaining DNA complement probes resulted in images c–e. The same region of the array is shown for all images. (see Colour Plate p. XXV).

Table 5.1 DNA sequences used in Figure 5.5.

Surface-bound probe DNA	*DNA sequences (5'–3'*
Probe A	TAC TCA CCC GTC CGC C
Probe B	CTT TTA TGT TTG AAC CAT GCG
Probe C	GTG GCC GAT CAC CCT CTC
Probe D	CGT GGC TTT CTG GTT A
Probe E	CTT TGA GTT TCA GTC

Probe DNA is modified with a 5'-thiol modifier and a 15-T spacer is appended to the 5' end of the probe DNA.

5.4.2
Mismatch Binding Protein, MutS

Mismatch binding proteins, such as MutS in *E. coli* are used by cells to identify and repair mismatches, short insertions, and deletions that are caused by replication errors. The ability to identify mismatches in DNA is necessary for the technology used to detect mutations and single nucleotide polymorphism in double-stranded DNA. Such assays may be important in the future for correlating genomic information from an individual with the development of diseases [24–26]. As an example, SPR imaging was used to show the interaction of MutS with mismatch DNA sequences (A–D) immobilized onto an array [9,27]. The sequences and additional experimental information are reported elsewhere [9]. This photopatterned array was exposed to a solution containing the sequence Z. Probe A did not hybridize with sequence Z and remained single stranded. Sequence Z formed a duplex with probe B containing a two-base insertion, a perfectly matched duplex with probe C, and a duplex containing a one-base G/T mismatch with probe D. Figure 5.6 shows an SPR difference image after MutS was allowed to bind to the DNA array. Adsorption of MutS was observed to both duplex B containing the insertion and duplex D containing the G/T mismatch, which has the strongest mismatch interaction with MutS [28]. Minimal binding occurred to the perfect match or the single-stranded DNA, showing that it was possible to study the sequence-specific interactions of MutS to DNA using SPR imaging measurements of DNA arrays. The utility of mismatch binding proteins to identify single-base mismatches, as well as short insertions and deletions in double-stranded DNA will lead to the application of mismatch binding proteins in mutation and single nucleotide polymorphism detection assays.

5.4.3
Bacterial Response Regulators, OmpR and VanR

Response regulators are DNA binding proteins that are essential components of the two-component signal transduction phosphorylation relay system used by bacteria to respond to environmental stimuli and to adapt accordingly through transcriptional activation of certain genes [29]. Since few response regulators have been studied in depth, DNA arrays are a potential tool to determine the DNA sequences recognized by a particular response regulator. As an example, the sequence-specific binding of two response regulators, OmpR and VanR, to DNA probe molecules was studied [30]. OmpR is one of the most well-characterized response regulators and is important in bacterial response to environmental osmotic pressure [31], while VanR is involved in the development of antibiotic resistance [32].

A photopatterned array was prepared containing six different immobilized DNA probes known to interact with either OmpR or VanR. The DNA array was then exposed to solutions of corresponding complementary DNA to create surface-immobilized double-stranded DNA. Figure 5.7a shows an SPR difference image after the array was exposed to a 100 nM solution of OmpR. OmpR primarily

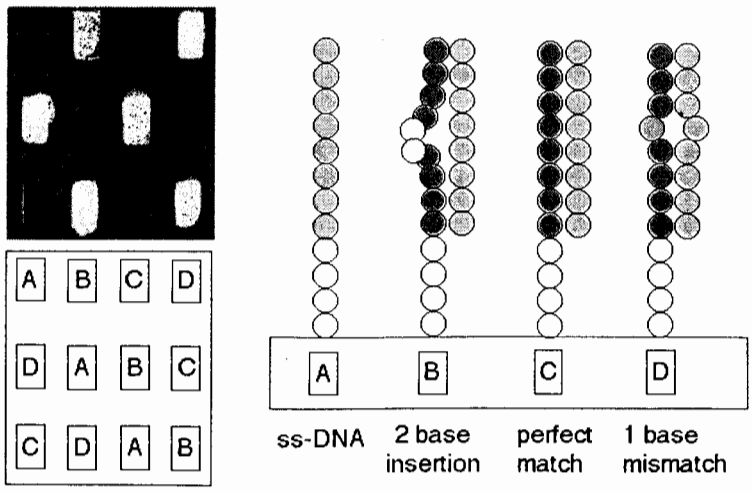

Figure 5.6 SPR imaging measurements of E. *coli* mismatch binding protein MutS adsorption onto a DNA array. This array was created with DNA probes A through D immobilized on 500 by 500 μm array elements in the pattern shown on the left of the figure. The array was then exposed to a solution containing the sequence Z. Z does not bind at all to probe A leaving it single strandedbut binds to probe B to create a duplex containing a two-base insertion, to probe C in a perfectly complementary manner, and to probe D to form a duplex containing a single-base mismatch. An SPR difference image of the binding of MutS to the array is shown on the right of the figure. The image shown is the difference between two images collected before and after exposure of the surface to MutS. Only 12 array elements from the total patterned surface area of 0.8 cm2 are presented in these images. Reprinted with permission from *Annual Review of Physical Chemistry* **51,** pp 41–63. Copyright 2000 by Annual Reviews www.annualreview.org. (see Colour Plate p. XXV).

absorbed to the DNA sequences OmpF1, F1F2, and C2 which were known to interact only with OmpR. The array was then regenerated with urea and exposed to complementary DNA before VanR (500 nM) was introduced to the array. VanR primarily bound to the DNA sequences VanH1, H2, and R1 (Figure 5.7b). Little nonspecific adsorption of either VanR or OmpR to the other sequences on the chip was observed. DNA probe sequences for VanR and OmpR response regulators can be found in the literature [30].

In addition to sequence specificity, SPR imaging measurements of DNA arrays can also be used to monitor inhibitor reactions that obstruct the binding of response regulators to DNA controlling gene expression in the bacteria. Figure 5.8 shows the effect of the inhibitor CpdA on VanR binding to the DNA sequences VanH1, H2, and R1 as measured by SPR imaging. The changes in percentage reflectivity were measured as a function of VanR concentration with and without 5 μM of CpdA. Integration of the line profile was performed to determine the average change in percentage reflectivity for the DNA sequences VanH1, H2, and R1. As can be seen in Figure 5.8, more adsorption is observed in the absence of the inhibitor than when CpdA is included with the VanR solution.

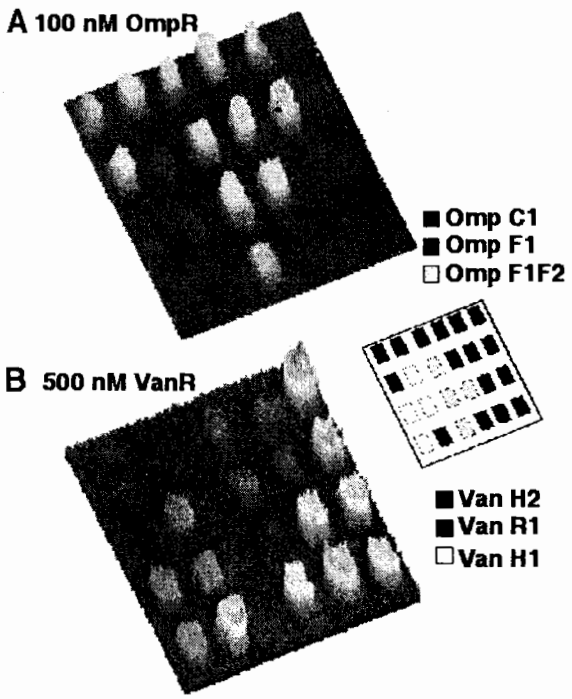

Figure 5.7 Surface plasmon imaging difference images of response regulator adsorption to double-stranded DNA immobilized on a photopatterned array composed of 500 by 500 μm array elements. (A) Specific adsorption of a 100 nM solution of OmpR to the DNA sequences OmpF1, F1F2, and C2. (B) VanR (500 nM) adsorbs to the DNA sequences VanH1, H2, and R1. OmpR is known to bind to the DNA sequences OmpF1, F1F2, and C2 and VanR is known to bind VanH1, H2, R1. There is little non-specific adsorption of the response regulators to the other sequences on the chip. DNA probe sequences for VanR and OmpR response regulators can be found in the literature. Reprinted with permission from *Langmuir*, Vol. 19, 1486–1492. Copyright 2003 American Chemical Society. (see Colour Plate p. XXVI).

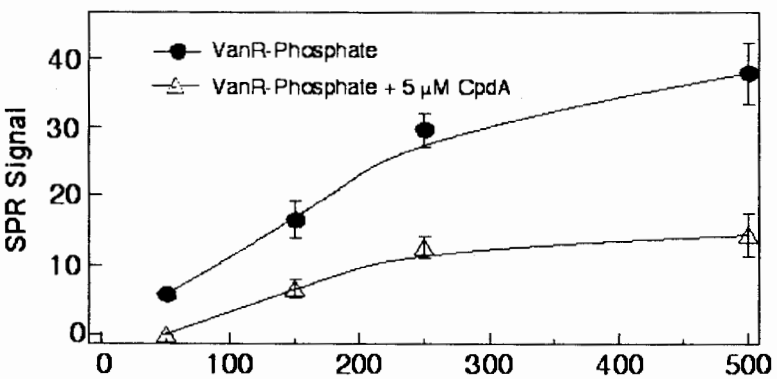

Figure 5.8 Plot showing the change in percentage reflectivity observed when VanR-phosphate (●) and VanR-phosphate plus 5 mM CpdA (○) adsorb to VanR DNA promoter sequences as a function of protein concentration. Integration of the line profile of VanR binding to DNA sequences VanH1, H2, and R1 was used to determine the average percentage reflectivity at each protein concentration. Less VanR-phosphate adsorbs to the DNA probes in the presence of the inhibitor CpdA than in its absence. Reprinted with permission from *Langmuir*, Vol. 19, 1486–1492. Copyright 2003 American Chemical Society.

5.5
SPR Imaging Experiments of Arrays Created by Microfluidic Stencils

We have recently developed a second fabrication and detection approach based on the coupling of microfluidic networks to SPR imaging measurements with the specific aim of lowering detection limits, reducing analysis time, and decreasing chemical consumption and sample volume [14]. This approach relies on the construction of microfluidic networks within the polymer polydimethylsiloxane (PDMS), which are physically sealed to chemically-modified gold surfaces. These PDMS microchannels were used in two ways: (i) to fabricate "1-D" arrays consisting of lines of immobilized peptides and DNA probes and (ii) to create "2-D" detection arrays in which a second set of PDMS microchannels were placed perpendicular to a 1-D line array in order to deliver target samples with small volume [14].

5.5.1
1-D Peptide Array for Antibody Binding Measurements

The fabrication of 1-D line arrays on gold surfaces is as follows. First, a set of parallel microchannels from PDMS were created by replication from 3-D silicon wafer masters that were created photolithographically from a 2-D chrome mask pattern (Figure 5.9) [33,34]. The microchannels were physically attached to a gold substrate modified with MUAM. A simple differential pumping system was used to introduce the chemical linkers SATP or SSMCC into the microchannels. Next, the DNA or peptide probe molecules were reacted within the microchannels. Once the immobilization was complete, the channels were removed and the alkanethiol-terminated monolayer was treated with PEG-NHS to prevent non-specific adsorption to the surface. Since the PDMS microchannels physically define where the probe molecules are immobilized, protection and deprotection chemistry is not required. By changing the spacing of the channels, up to 100 different peptide or DNA sequences can be immobilized on one chip. The array can then be coupled with a large volume flow cell (500 μL) to introduce analytes to the line array.

SPR imaging measurements were used to monitor the sequence-specific adsorption of antibodies to a two-component peptide array. The linear array contained the peptide sequences, Myc and HA denoted A and B, respectively (Figure 5.10). The introduction of a 25 nM solution of anti-Myc though a 500 μL flow cell resulted in specific adsorption to probe A. The anti-Myc was removed from the surface using pH 11.5 buffer prior to exposing the array to a solution of 100 nM anti-HA. Anti-HA primarily bound to probe B, although some non-specific adsorption probe A was observed.

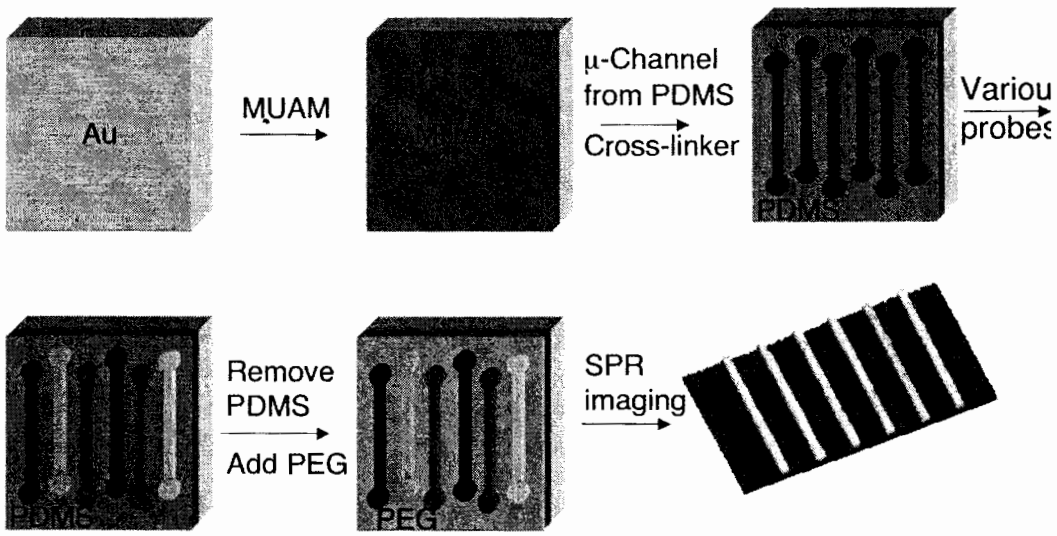

Figure 5.9 Schematic representation of the microfabrication strategy used to create DNA, peptide and protein linear arrays. A self-assembled monolayer of MUAM was formed on a clean gold surface. Polydimethyl siloxane (PDMS) microchannels were used to deliver bifunctional linkers and probe biomolecules to the surface. The microchannels were removed and the background was protected with a polyethylene glycol derivative. Adapted with permission from *Analytical Chemistry*, **73** 5525–5531. Copyright 2001 American Chemical Society. (see Colour Plate p. XXVI).

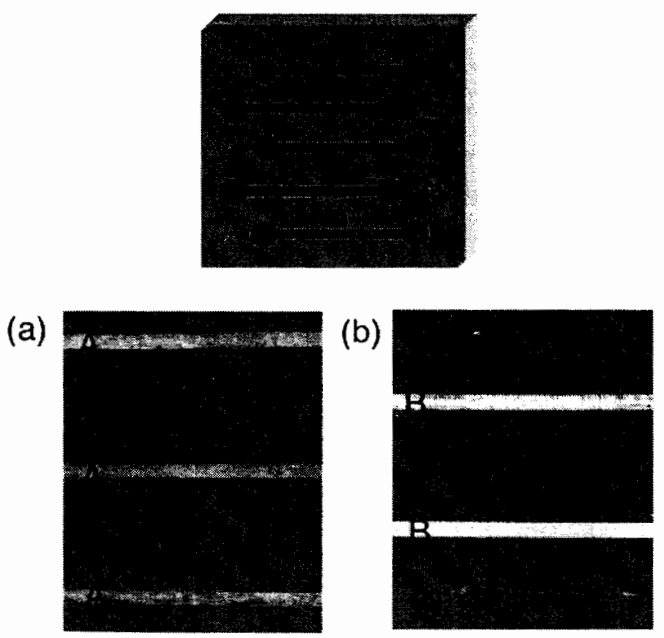

Figure 5.10 SPR difference images showing the sequence-specific binding interactions of antibodies to a peptide linear array containing two probes A and B corresponding to the peptide sequences Myc and HA. The peptides were immobilized in the pattern shown in the figure. (a) First, the array was exposed to a 25 nM solution of anti-Myc. Specific adsorption of anti-Myc to probe A is observed. (b) After rinsing with pH 11.5 buffer to regenerate the surface, the experiment was repeated 100 nM anti-HA. Anti-HA primarily bound to probe B, with little non-specific interaction with probe A. (see Colour Plate p. XXVII).

5.5.2. 2-D DNA Array for RNA Hybridization

In a second approach, microfluidic channels were used as a small volume flow cell during SPR imaging measurements to reduce the required analyte and to simultaneously introduce multiple analytes. First, a 1-D array composed of DNA elements was prepared and the background protected with PEG. Then a second set of PDMS channels was placed perpendicular to the immobilized DNA lines, forming a 2-D array, and used to introduce analytes to the array surface during SPR imaging experiments (Figure 5.11a). Figure 5.11b shows the schematic diagram of an SPR imager set-up where the large flow cell (500 μL) has been replaced with microfluidic channels constructed in PDMS reducing the required sample volume to 1 μL. An example of an SPR difference image of a three-component 2-D hybridization DNA array exposed to GUS gene ssRNA through PDMS microchannels is shown in Figure 5.12. About 20 femtomoles of RNA in a total solution volume of 1 μL was delivered through each channel. The DNA sequences and more information are reported elsewhere [14]. Varying SPR signal intensities were observed for the three different probes in Figure 5.12 and can be attributed to differences in the binding efficiency of the *GUS* gene ssRNA to the different surface-bound ssDNA probes. The ability to detect 20 femtomoles of ssRNA is sufficient for a number of biological applications, including the direct detection of messenger RNA (mRNA) from highly expressed genes and the detection of ribsomal RNA (rRNA) from complex biological samples.

5.5.3 2-D Peptide Array for Antibody Binding Measurements

SPR imaging technology integrating microfluidics was applied to monitor the sequence-specific interactions of antibodies to peptide motifs for epitope mapping applications. For example, peptide arrays were used to study the residues essential to the binding motif of anti-FLAG M2, an antibody commonly used for the purification of fusion proteins [35]. SPR imaging is currently used to study cell adhesion processes and to investigate the enzymatic modifications of peptides by sequence-specific phophatases, kinases, and proteases. Ultimately, these techniques could be used to identify the important residues in previously uncharacterized protein–protein interactions based on peptide recognition motifs.

Sequence-specific adsorption of anti-FLAG M2 to four different peptide epitopes based on the FLAG peptide tag was studied with SPR imaging [10]. Peptide line arrays were created using a microfluidic fabrication process and coupled to a second microchannel with a wraparound design (Figure 5.13a). The "worm" microchannel has a total sample volume of 5 μL and is used to deliver antibody to the peptide array. Figure 5.13b shows a difference image obtained by subtracting images of a fourcomponent peptide array before and after the introduction of a solution of 100 nM anti-FLAG M2. A line profile taken across the channels indicated that the greatest amount of antibody adsorption is observed at elements where

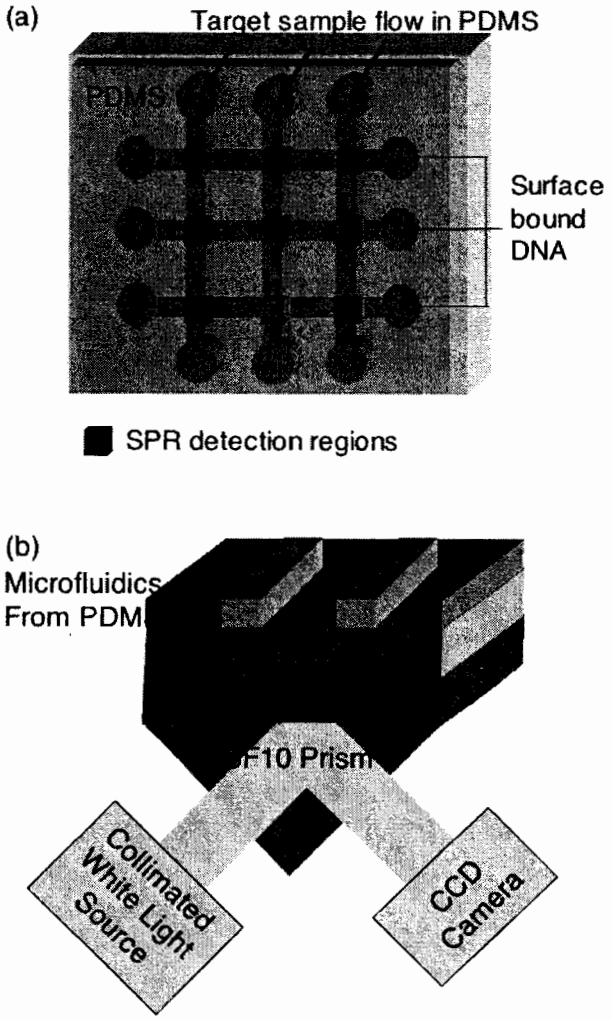

Figure 5.11 (a) Schematic diagram of parallel polydimethyl siloxane (PDMS) microchannels used to deliver small volumes of analyte (1 µl) to peptide and DNA linear arrays.
(b) Schematic representation of the SPR imaging experimental set-up incorporating PDMS microfluidics to deliver a small volume of target sample. This configuration allows different analytes to be delivered through each channel. (see Colour Plate p. XXVIII).

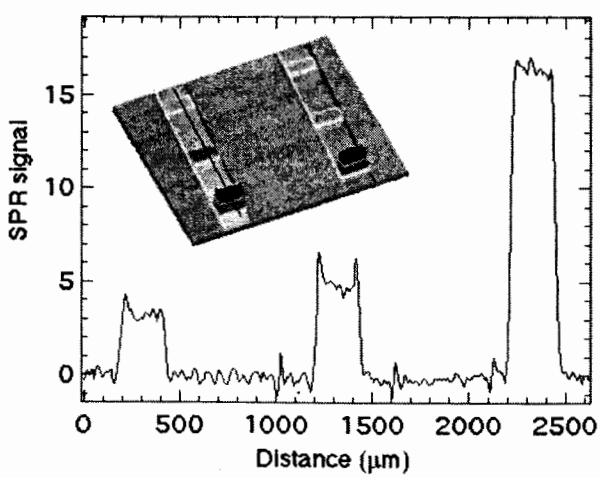

Figure 5.12 An SPR difference image showing adsorption of GUS gene ssRNA onto DNA probes. Each channel was 300 µm wide, 35 µm deep, and 1.2 µm long with 900 µm spacing between channels. Reprinted with permission from *Analytical Chemistry*, **73** 5525–5531. Copyright 2001 American Chemical Society. (see Colour Plate p. XXIX).

the original sequence, F1, was immobilized. The least amount of binding was observed to the peptide sequences F3 and F4. These peptides differed from the original sequence by the substitution of an amino acid important to the binding motif by an alanine residue. In contrast to the F3 and F4 peptides, the F2 sequence had a substantially higher signal, since this peptide contained an alanine substitution for a non-essential residue in the binding motif. These data demonstrate that SPR imaging can be used to compare the amount of protein binding to peptides differing by a single amino acid and to determine the importance of each residue for a peptide–protein interaction.

Quantitative SPR imaging measurements can also be used to simultaneously determine adsorption constants for the interactions of antibodies with multiple peptide motifs on a single chip [10]. The change in percentage reflectivity was measured for the peptide sequences F1 and F2 at increasing antibody concentrations. This data is shown in Figure 5.14 where the SPR signal resulting from antibody adsorption is plotted as a function of anti-FLAG M2 concentration, ranging from 1 to 150 nM. These data points were fitted with a Langmuir isotherm. The adsorption constants were found to be 1.5×10^8 M^{-1} for F1 and 2.8×10^7 M^{-1} for F2, showing that the original sequence had a stronger antibody peptide interaction. The detection limit for the F1 peptide with anti-FLAG M2 was 0.5 nM.

5.5.4
2-D Protein Array

With the sequencing of many genomes complete, it has become clear that high-throughput methods for studying gene products is necessary in order to elucidate the vast amount of information encoding biological function in an organism. Such studies would be enhanced by the addition of label-free analytical tools such as SPR imaging. The utility of SPR imaging for the study of protein–peptide interactions demonstrated the feasibility of this technique for measuring the adsorption of biomolecules to immobilized proteins. The first step for adapting SPR imaging measurements to the study of protein–protein interactions is the creation of a robust reproducible, biologically-active protein array. Most protein arrays are constructed by random attachment strategies, using naturally occurring lysines and terminal amines for surface attachment [36]. However, such approaches have the potential to interfere with the binding site of the protein, negatively affecting biological activity. To target such problems, we have established a general methodology to create oriented arrays of fusion proteins attached to gold thin films. In an oriented fusion protein array, the fusion protein or tag will interact with a capture agent immobilized on the gold thin film leaving the protein of interest free to interact with proteins in solution. We are currently investigating several fusion protein/capture agent pairs including the histidine peptide tag with NTA [37–39], glutathione S-transferase (GST) with glutathione or anti-GST [40,41], and maltose binding protein (MBP) with maltose [42,43]. Since these tags and capture agents are commonly used for the purification of fusion proteins, they are well-character-

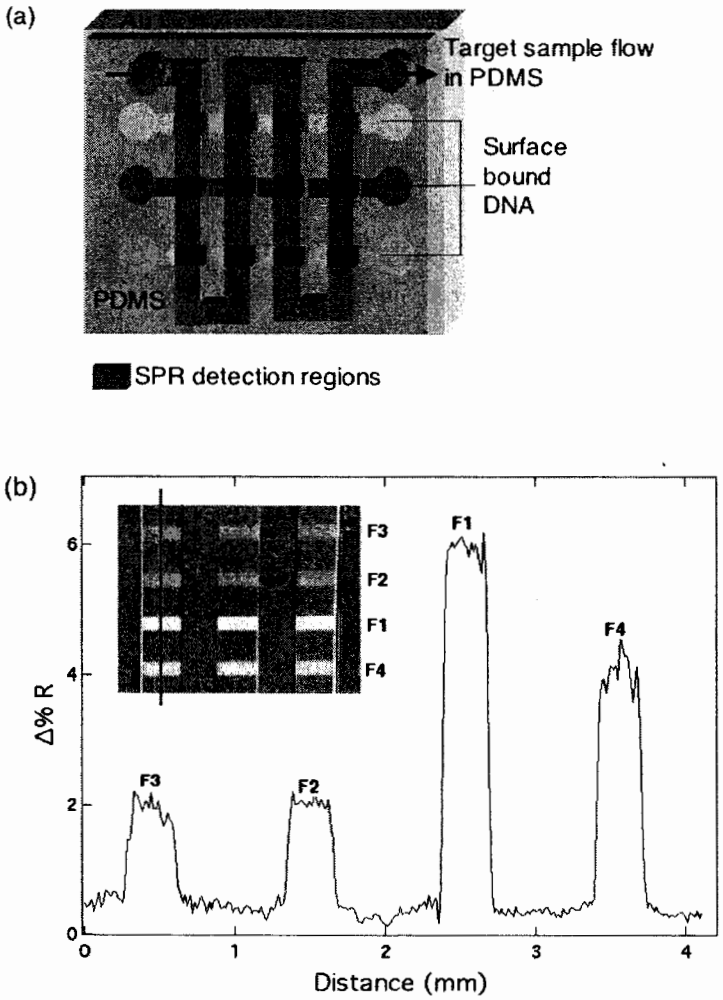

Figure 5.13 (a) A worm microchannel is used to deliver 5 μl aliquots of antibody solution to the peptide linear array. This microfluidic configuration is suitable for the delivery of a small volume of a single analyte to the array with a detection area equivalent to a configuration using a large volume flow cell. The worm channel was 500 μm wide, 35 μm deep, and 12 mm long with 500 μm spacing between channels.
(b) SPR difference image showing the adsorption of 100 nM anti-FLAG to a peptide array composed of four epitopes, differing by a single amino acid, based on the FLAG peptide sequence. The line profile reveals that the greatest adsorption occurs at elements containing the original sequence, F1. Diminished adsorption is observed at sequences, F3 and F4, containing alanine substitutions for essential residues of the binding motif. Peptide probe sequences can be found in the literature. Reprinted with permission from *Analytical Chemistry*, **74,** 5161–5168. Copyright 2002 American Chemical Society. (see Colour plate p. XXIX).

ized and the proteins can be released to follow up SPR imaging measurements with further off-chip solution phase experiments.

Protein arrays fabricated using NTA-modified gold films to capture his-tagged proteins are a promising tool for the study of protein–protein interactions using SPR imaging (see Figure 5.15a). A worm microchannel was used to pattern a self-assembled alkanethiol monolayer on a gold thin film with NTA capture agents. This microchannel was then removed and the whole surface was reacted with a polyethylene glycol derivative to prevent the non-specific adsorption of proteins to

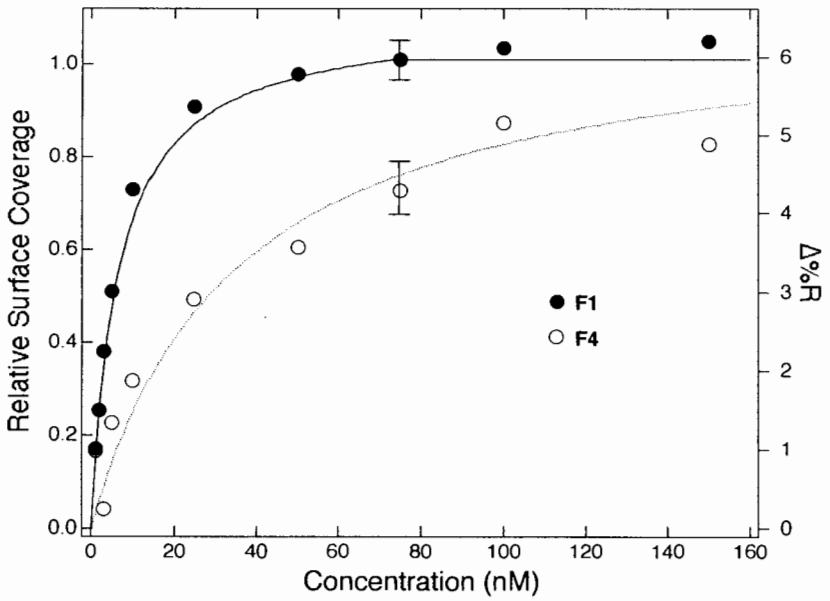

Figure 5.14 Langmuir isotherms fitted to the adsorption of anti-FLAG M2 onto an array containing the peptides F1 (●) and F2 (○). The change in percentage reflectivity was determined by integrating the line profiles for the F1 and F2 peptides at varying anti-FLAG M2 concentrations. The adsorption constants were calculated by the fit of the Langmuir isotherms, to be 1.5×10^8 M^{-1} and 2.8×10^7 M^{-1} for F1 and F4 respectively. Reprinted with permission from *Analytical Chemistry*, **74**, 5161–5168. Copyright 2002 American Chemical Society.

the background around the NTA capture agents. Next a second set of parallel microchannels oriented perpendicular to the immobilized NTA lines was used to introduce proteins to the surface (Figure 5.15b). This fabrication method provides a convenient and fast way to create arrays composed of one protein per channel. As shown in the SPR difference image in Figure 5.15c, both polyhistidine and histidine-tagged ubiquitin interact with the NTA surfaces in the presence of nickel ions, while little adsorption of these biomolecules is observed when nickel ions are not present, showing the specificity of the interaction. This protein fabrication strategy has the advantage that SPR imaging measurements can be used to evaluate protein immobilization onto the array prior to using the chip to study protein–protein interactions. Our current efforts are focused on the application of SPR imaging measurements to study the interactions of protein, DNA, and peptides to protein chips. Initial results indicate the SPR imaging techniques will become an innovative tool for proteomics research.

5.6 Conclusions

SPR imaging is emerging as a promising tool for the study of bioaffinity interactions in an array format. This review presented various recent applications of SPR imaging measurements for the study of DNA, RNA, and protein interactions with

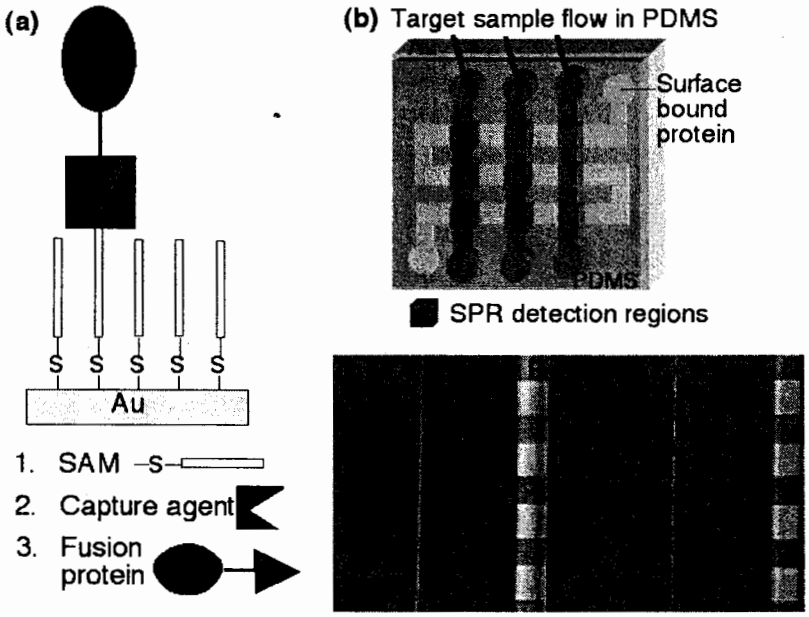

Figure 5.15 (a) Schematic representation of a general approach for the creation of an oriented fusion protein array on gold surfaces. (b) The NTA capture agent was immobilized through a worm microchannel. Next, a parallel set of PDMS channels was used to simultaneously deliver multiple histidine-tagged analytes to the NTA elements. (c) An example of an SPR difference image showing the immobilization of histidine-tagged ubiquitin **B** and polyhistidine D to NTA-modified monolayers in the presence of nickel ions. In the absence of nickel ions there is little non-specific adsorption of his-tagged ubiquitin **A** or polyhistidine **C** to the NTA surface, suggesting that a specific chelation interaction is occurring. (see Colour Plate p. XXX).

biomolecular arrays. The key components for these experiments are a well-characterized chemical modification of gold thin films to immobilize biomolecular probe molecules coupled with a robust array fabrication method based on photopatterning or microfluidics. The development of two different methods of array fabrication has increased the versatility of the SPR imaging technique; the linear arrays created from microfluidics are particularly efficient in terms of time and materials for arrays requiring only a small number (< 100) of different surface-bound biomolecules, whereas the generalized photopatterned array fabrication methodology is more applicable to systems where the number of surface-attached biomolecules is greater than 100. The successful application of DNA, peptide, and carbohydrate arrays to study protein binding interactions demonstrates the wide variety of bioaffinity interactions that can be observed with SPR imaging. The study of protein–protein interactions by SPR imaging is still in its infancy, but we predict that this technology will have a significant role to play in the high-throughput screening of protein–protein interactions, the study of synthetic chemical libraries, the binding and inhibition of cell receptors, and the elucidation of regulatory pathways in biological systems.

Acknowledgments

This research is funded by the National Institute of Health (3R01 GM59622-03S 1 and 8 ROI EB00269-02) and the National Science Foundation (CHE-0133151).

References

1. Miller, J. C., Butler, E. B., Teh, B. S., Haab, B. B. The application of protein microarrays to serum diagnostics: Prostate cancer as a test case. *Disease Markers* 2001, **17,** 225–234.
2. Zhu, H., Klemic, J. F., Chang, S., Bertone, P., Casamayor, A., Klemic, K. G., Smith, D., Gerstein, M., Reed, M. A., Snyder, M. Analysis of yeast protein kinases using protein chips. *Nature Genet.* 2000, **26,** 283–289.
3. Zhu, H., Bilgin, M., Bangham, R., Hall, D., Casamayor, A., Bertone, P., Lan, N., Jansen, R., Bidlingmaier, S., Houfek, T., Mitchell, T., Miller, P., Dean, R. A., Gerstein, M., Snyder, M. Global analysis of protein activities using proteome chips. *Science* 2001, **293,** 2101–2105.
4. Laune, D., Molina, F., Mani, J.-C., Del Rio, M., Bouanani, M., Pau, B., Granier, C. Dissection of an antibody paratope into peptides discloses the idiotope recognized by the cognate anti-idiotypic antibody. *J. Immun. Methods* 2000, **239,** 63–73.
5. Uthaipibull, C., Aufiero, B., Syed, S. E. H., Hanse, B., Guevara Patino, J. A., Angov, E., Ling, I. T., Fegerding, K., Morgan, W. D., Ockenhouse, C., Birdsall, B., Feeney, J., Lyon, J. A., Holder, A. A. Inhibitory and blocking monoclonal antibody epitopes on merozite surface protein 1 of the malaria parasiste plasmodium falciparum. *J. Mol. Biol.* 2001, **307,** 1381–1394.
6. Houseman, B. T., Huh, J. H., Kron, S., J., Mrksich, M. Peptide chips for the quantitative evaluation of protein kinase activity. *Nature Biotech.* 2001, **20,** 270–274.
7. Kilpert, K., Hansen, G., Wessner, H., Schneider-Mergener, J., Hohne, W. Characterizing and optimizing protease/peptide inhibitor interactions, a new application for spot synthesis. *J. Biochem.* 2000, **128,** 1051–1057.
8. Brockman, J. M., Frutos, A. G., Corn, R. M. A multi-step chemical modification procedure to create DNA arrays on gold surfaces for the study of protein–DNA interactions with surface plasmon resonance imaging. *J. Am. Chem. Soc.* 1999, **121,** 8044–8051.
9. Frutos, A. G., Brockman, J. M., Corn, R. M. Reversible protection and reactive patterning of amine- and hydroxyl-terminated self-assembled monolayers on gold surfaces for the fabrication of biopolymer arrays. *Langmuir* 2000, **16,** 2192–2197.
10. Wegner, G. J., Lee, H. J., Corn, R. M. Characterization and optimization of peptide arrays for the study of epitope–antibody interactions using surface plasmon resonance imaging. *Anal. Chem.* 2002, **74,** 5161–5168.
11. Nelson, B. P., Frutos, A. G., Brockman, J. M., Corn, R. M. Near-infrared surface plasmon resonance measurements of ultrathin films. 1. Angle shift and SPR imaging experiments. *Anal. Chem.* 1999, **71,** 3928–3934.
12. Hansen, W. N. Electric fields produced by the propagation of plane coherent electromagnetic radiation in a stratified medium. *J. Opt. Soc. Am.* 1968, **58,** 380–390.
13. Nelson, B. P., Grimsrud, T. E., Liles, M. R., Goodman, R. M., Corn, R. M. Surface plasmon resonance imaging measurements of DNA and RNA hybridization adsorption onto DNA microarrays. *Anal. Chem.* 2001, **73,** 1–7.
14. Lee, H. J., Goodrich, T. T., Corn, R. M. SPR imaging measurements of 1-D and 2-D DNA microarrays created from microfluidic channels on gold thin films. *Anal. Chem.* 2001, **73,** 5525–5531.
15. Pease, A. C., Solas, D., Sullivan, E. J., Cronin, M. T., Holmes, C. P., Fodor, S. P. A. Light-generated oligonucleotide arrays for rapid DNA sequence analysis. *Proc. Natl Acad. Sci. USA* 1994, **91,** 5022–5026.
16. Schena, M., Shalon, D., Davis, R. W., Brown, P. O. Quantitative monitoring of gene expression patterns with a complementary DNA microarray. *Science* 1995, **270,** 467–470.
17. Brenner, S., Johnson, M., Bridgham, J., Golda, G., Lloyd, D. H., Johnson, D., Luo, S., McCurdy, S., Foy, M., Ewan, M., Roth, R., George, D., Eletr, S., Albrecht, G., Vermaas, E., Williams, S. R., Moon, K., Burcham, T., Pallas, M., DuBridge, R. B., Kirchner, J., Fearon, K., Mao, J., Corcoran, K. Gene expression analysis by massively parallel signature sequencing (MPS) on microbead arrays. *Nature Biotech.* 2000, **18,** 630–634.

18. Winzeler, E. A., Richards, D. R., Conway, A. R., Goldstein, A. L., Kalman, S., McCullough, M. J., McCusker, J. H., Stevens, D. A., Wodicka, L., Lockhart, D. J., Davis, R. W. Direct allelic variation scanning of the yeast genome. *Science* 1998, **281,** 1194–1197.
19. Wenschuh, H., Volkmer-Engert, R., Schmidt, M., Schulz, M., Schneider-Mergener, J., Reineke, U. Coherent membrane supports for parallel microsynthesis and screening of bioactive peptides. *Biopolymers* 2000, **55,** 188–206.
20. Frank, R. Spot-synthesis: An easy technique for the positionally addressable, parallel chemical synthesis on a membrane support. *Tetrahedron* 1992, **48,** 9217–9232.
21. Reineke, U., Volkmer-Engert, R., Schneider-Mergener, J. Applications of peptide arrays prepared by the SPOT-technology. *Curr. Opin. Biotech.* 2001, **12,** 59–64.
22. Frey, B., Corn, R. M. Covalent attachment and derivitization of poly(L-lysine) monolayers on gold surfaces as characterized by polarization-modulation FT-IR spectroscopy. *Anal. Chem.* 1996, **68,** 3187–3193.
23. Smith, E., Wanat, M. J., Cheng, Y., Barreira, S. V. P., Frutos, A. G., Corn, R. M. Formation, spectroscopic characterization, and applications of sulfhydryl-terminated alkanethiol monolayers for the chemical attachment of DNA onto gold surfaces. *Langmuir* 2001, **17,** 2502–2507.
24. Hirschhorn, J. N., Sklar, P., Lindblad-Toh, K., Lim, Y. M., Ruiz-Gutierrez, M., Bolk, S., Langhorst, B., Schaffer, S. E., Winchester, E., Landler, E. S. SBE-TAGS: An array-based method for efficient single-nucleotide polymorphism genotyping. *Proc. Natl Acad. Sci. USA* 2000, **97,** 12164–12169.
25. Reich, D. E., Cargill, M., Bolk, S., Ireland, J., Sabeti, P. C., Richter, D. J., Lavery, T., Kououmjian, R., Farhadian, S. F., Ward, R., Lander, E. S. Linkage disequilibrium in the human genome. *Nature* 2001, **411,** 199–204.
26. Brookes, A. J. The essence of SNPs. *Gene* 1999, **234,** 177–186.
27. Brockman, J. M., Nelson, B. P., Corn, R. M. Surface plasmon resonance imaging measurements of ultrathin organic films. *Annu. Rev. Phys. Chem.* 2000, **51,** 41–63.
28. Su, S. S., Lahue, R. S., Au, K. G., Modrich, P. Mispair Specifity of Methy-directed DNA Mismateh Correction *in vitro*. *J. Biol. Chem.* 1987, **263,** 6829–6835.
29. Hoch, J. A. Two component and phosphorelay signal transduction. *Curr. Opin. Microbiol.* 2000, **3,** 165–170.
30. Smith, E. A., Erickson, M. G., Ulijasz, A. T., Weisblum, B., Corn, R. M. Surface plasmon resonance imaging of transcription factor proteins: interactions of bacterial response regulators with DNA arrays on gold films. *Langmuir* 2003, **19,** 1486–1492.
31. Martinez-Hackert, E., Stock, A. M. Structural relationships in the OmpR family of winged-helix transcription factors. *J. Mol. Biol.* 1997, **269,** 301–312.
32. Haldimann, A., Fisher, S. L., Daniels, L. L., Walsh, C. T., Wanner, B. L. Transcriptional regulation of the *Enterococcus faecium* BM4147 vancomycin resistance gene cluster by the VanS-VanR two-component regulatory system in *Escerichia coli* K-12. J. *Bacteriol.* 1997, **179,** 5903–5913.
33. Jackman, R. J., Duffy, D. C., Ostuni, E., Willmore, N. D., Whitesides, G. M. Fabricating large arrays of microwells with arbitrary dimensions and filling them using discontinuous de-wetting. *Anal. Chem.* 1998, **70,** 2280–2287.
34. Duffy, D. C., McDonald, J. C., Schueller, O. J. A., Whitesides, G. M. Rapid prototyping of microfluidic systems in poly(dimethylsiloxane). *Anal. Chem.* 1998, **70,** 4974–4984.
35. Slootstra, J. W., Kuperus, D., Pluckthun, A., Meloen, R. H. Identification of new tag sequences with differential and selective recognization properties for the anti-FLAG monoclonal antibodies M1, M2, and M5. *Mol. Divers.* 1996, **2,** 156–164.
36. Schreiber, S. L., MacBeath, G. Printing proteins as microarrays for high-throughput function determination. *Science* 2000, **289,** 1760–1763.
37. Bornhorst, J. A., Falke, J. J. Purification of proteins using polyhistidine affinity tags. *Methods Enzymol.* 2000, **326,** 245–254.
38. Schmitt, J., Hess, J., Stunnenberg, H. G. Affinity purification of histidine-tagged proteins. *Mol. Biol. Rep.* 1993, **18,** 223–230.

39. Ho, C. H., Limberis, L., Caldwell, K. D., Stewart, R. J. A meta-chelating pluronic for immobilization of histidine-tagged proteins at interfaces: Immoblilization of firefly luciferase on polystyrene beads. *Langmuir* 1998, **14,** 3889–3894.

40. Simons, P. C., Vander Jagt, D. L. Purification of glutathione S-transferase from human liver by glutathione-affinity chromatography. *Anal. Biochem.* 1977, **82,** 334–341.

41. Wang, C., Castro, A. F., Wilkes, D. M., Altenberg, G. A. Expression and purification of the first nucleotide-binding domain and linker region of human multidrug resistance gene product: Comparison of fusions to glutathione S-transferase, thioredoxin and maltose-binding protein. *Biochem. J.* 1999, **338,** 77–81.

42. Cattoli, F., Sarti, G. C. Separation of MBP fusion proteins through affinity membranes. *Biotechnol. Prog.* 2002, **18,** 94–100.

43. Bach, H., Mazor, Y., Shaky, S., Shoham-Lev, A., Berdichevsky, Y., Gutnick, D. L., Benhar, I. Escherichia coli maltose-binding protein as a molecular chaperone for recombinant intracellular cytoplasmic single-chain antibodies. *J. Mol. Biol.* 2001, **312,** 79–93.

Chapter 5

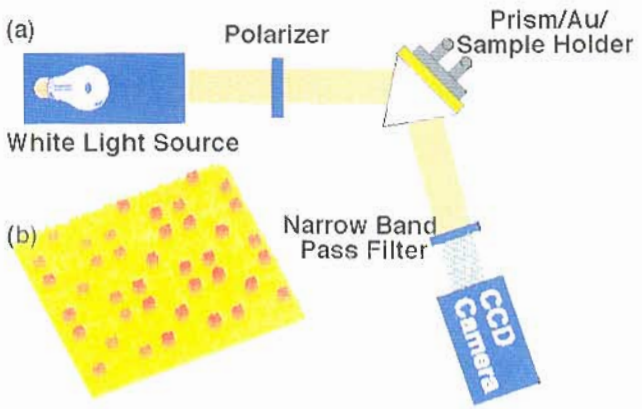

Figure 5.2 Schematic diagram of the surface plasmon imager apparatus. P-polarized white light impinges on a prism sample apparatus at a fixed optimal angle, near the surface plasmon angle. The light is then passed through a narrow band pass filter and images are collected by a CCD camera. The analyte is delivered to the array fabricated on a gold thin film using a simple 500 μL flow cell. An SPR difference image of the sequence-specific hybridization of 18-mer DNA to a two-component DNA array is shown in the bottom left corner of the figure. A maximum of 160 array elements can be studied on one SPR chip with a total surface area of 0.8 cm^2 using square elements with 500 μm widths.

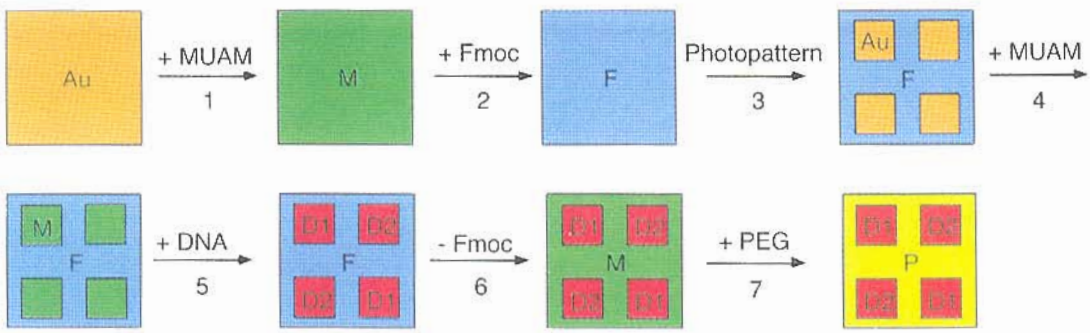

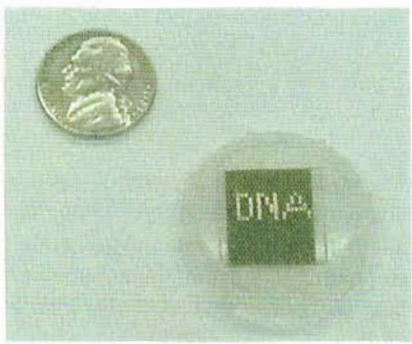

Au Bare Gold

M MUAM (amine terminated)

F Fmoc (hydrophobic)

D1 DNA or peptides attached with SSMCC or SATP

P PEG (resists protein adsorption)

Figure 5.4 Multi-step array fabrication process using protection/deprotection chemistry and photopatterning techniques to prepare DNA and peptide arrays. The bottom left corner of the figure shows individually addressable hydrophilic drops of DNA pinned to the surface by a hydrophobic background. First, a bare gold surface is modified with a self-assembled monolayer of 11-mercapto-undecylamine (MUAM). This amine-terminated surface is reacted with the hydrophobic protecting group Fmoc. UV-light is used to break the gold–thiol bond and create bare gold pads on the surface. These pads are subsequently filled with MUAM. A bifunctional linker is used to attach DNA or peptide probes to create an array. Finally, the Fmoc is removed with base and replaced with a polyethylene derivative to prevent the non-specific adsorption of biopolymers to the background. Reprinted with permission from *Journal of the American Chemical Society*, **121**, 8044–8051. Copyright 1999 American Chemical Society.

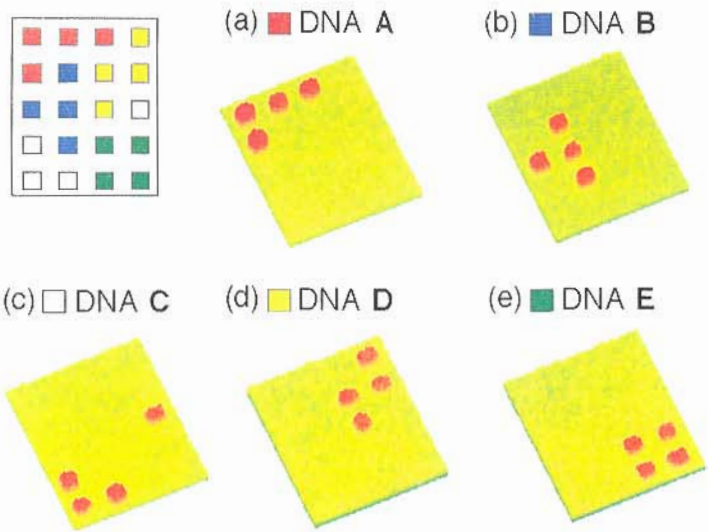

Figure 5.5 SPR difference images showing the hybridization of perfect-match DNA complements to a DNA array containing five different probes. The sequences were immobilized on 500 by 500 μm array elements in the pattern shown in the figure. (a) First, the array was exposed to a 100 nM solution of the DNA complement to probe A for 15 min. Hybridization adsorption onto the array is indicated by a change in the percentage reflectivity of incident light. (b) After rinsing with 8 M urea to regenerate the surface, the experiment was repeated with the DNA complement of probe B. Successive rounds of denaturation and hybridization of the remaining DNA complement probes resulted in images c–e. The same region of the array is shown for all images.

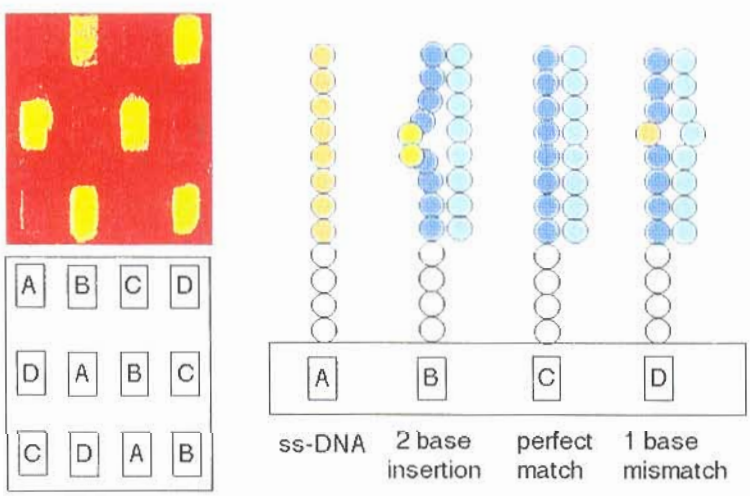

Figure 5.6 SPR imaging measurements of E. *coli* mismatch binding protein MutS adsorption onto a DNA array. This array was created with DNA probes A through D immobilized on 500 by 500 μm array elements in the pattern shown on the left of the figure. The array was then exposed to a solution containing the sequence Z. Z does not bind at all to probe A leaving it single strandedbut binds to probe B to create a duplex containing a two-base insertion, to probe C in a perfectly complementary manner, and to probe D to form a duplex containing a single-base mismatch. An SPR difference image of the binding of MutS to the array is shown on the right of the figure. The image shown is the difference between two images collected before and after exposure of the surface to MutS. Only 12 array elements from the total patterned surface area of 0.8 cm2 are presented in these images. Reprinted with permission from *Annual Review of Physical Chemistry* 51, pp 41–63. Copyright 2000 by Annual Reviews www.annualreview.org.

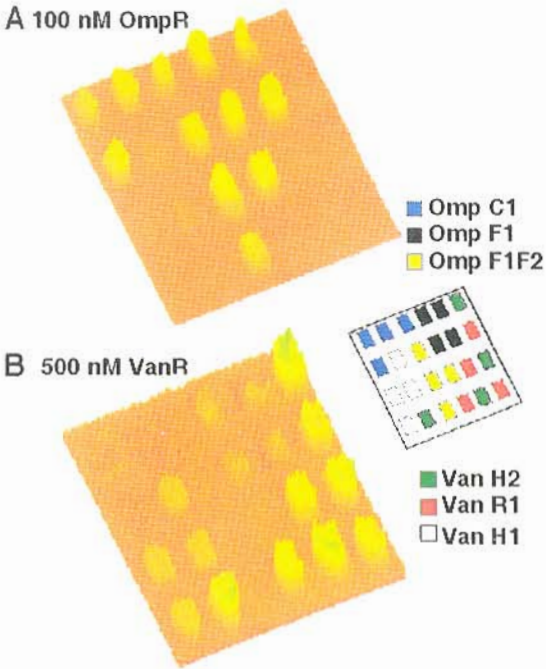

Figure 5.7 Surface plasmon imaging difference images of response regulator adsorption to double-stranded DNA immobilized on a photopatterned array composed of 500 by 500 μm array elements. (A) Specific adsorption of a 100 nM solution of OmpR to the DNA sequences OmpF1, F1F2, and C2. (B) VanR (500 nM) adsorbs to the DNA sequences VanH1, H2, and R1. OmpR is known to bind to the DNA sequences OmpF1, F1F2, and C2 and VanR is known to bind VanH1, H2, R1. There is little non-specific adsorption of the response regulators to the other sequences on the chip. DNA probe sequences for VanR and OmpR response regulators can be found in the literature. Reprinted with permission from *Langmuir*, Vol. 19, 1486–1492. Copyright 2003 American Chemical Society.

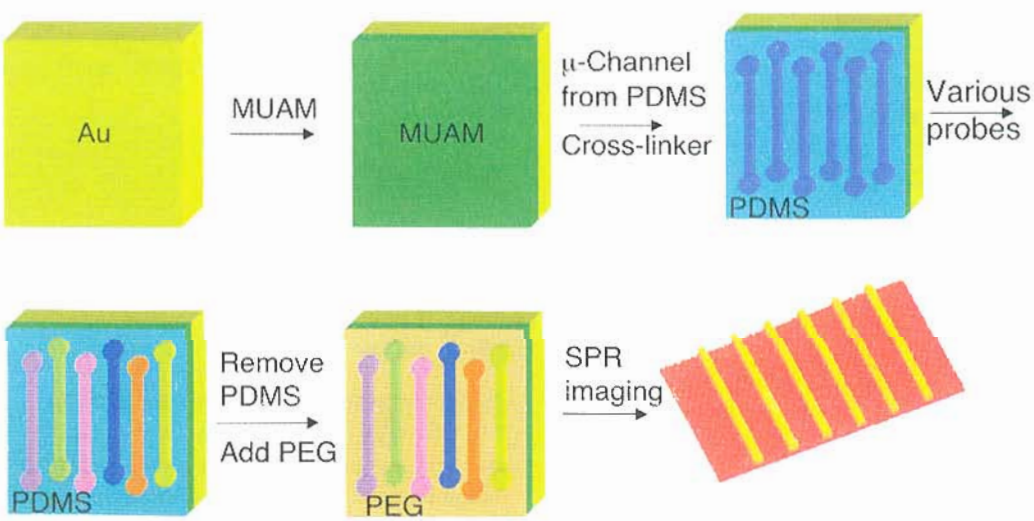

Figure 5.9 Schematic representation of the microfabrication strategy used to create DNA, peptide and protein linear arrays. A self-assembled monolayer of MUAM was formed on a clean gold surface. Polydimethyl siloxane (PDMS) microchannels were used to deliver bifunctional linkers and probe biomolecules to the surface. The microchannels were removed and the background was protected with a polyethylene glycol derivative. Adapted with permission from *Analytical Chemistry*, **73** 5525–5531. Copyright 2001 American Chemical Society.

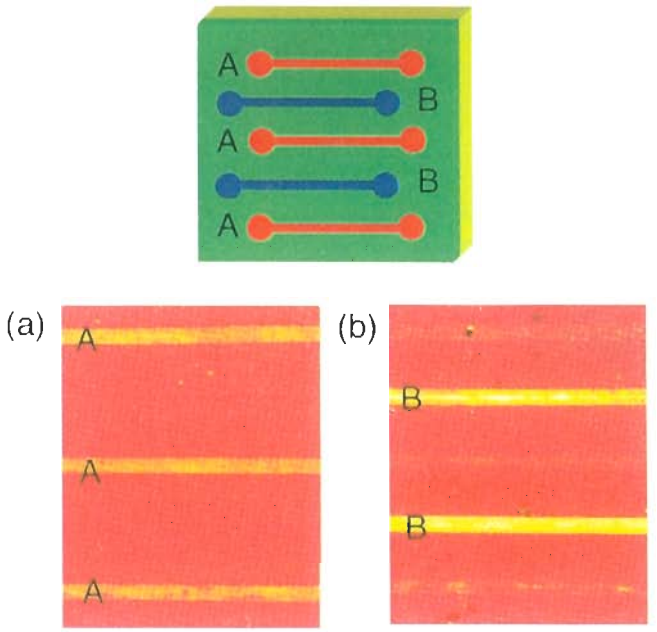

Figure 5.10 SPR difference images showing the sequence-specific binding interactions of antibod ies to a peptide linear array containing two probes A and B corresponding to the peptide sequences Myc and HA. The peptides were immobilized in the pattern shown in the figure. (a) First, the array was exposed to a 25 nM solution of anti-Myc. Specific adsorption of anti-Myc to probe A is observed. (b) After rinsing with pH 11.5 buffer to regenerate the surface, the experiment was repeated 100 nM anti-HA. Anti-HA primarily bound to probe B, with little non-specific interac- tion with probe A.

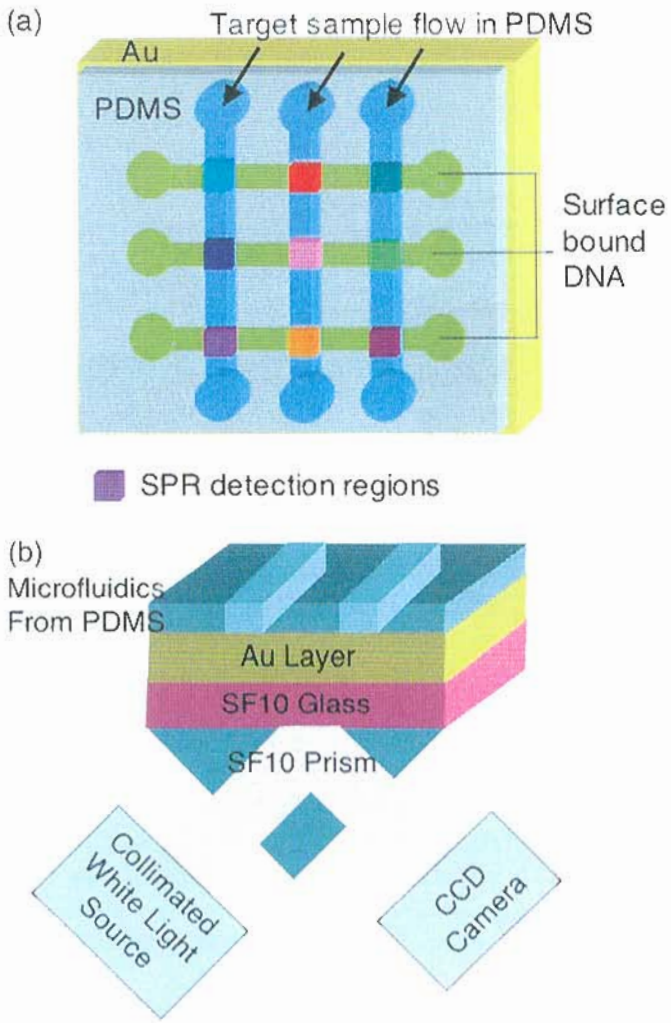

Figure 5.11 (a) Schematic diagram of parallel polydimethyl siloxane (PDMS) microchannels used to deliver small volumes of analyte (1 μl) to peptide and DNA linear arrays. (b) Schematic representation of the SPR imaging experimental set-up incorporating PDMS microfluidics to deliver a small volume of target sample. This configuration allows different analytes to be delivered through each channel.

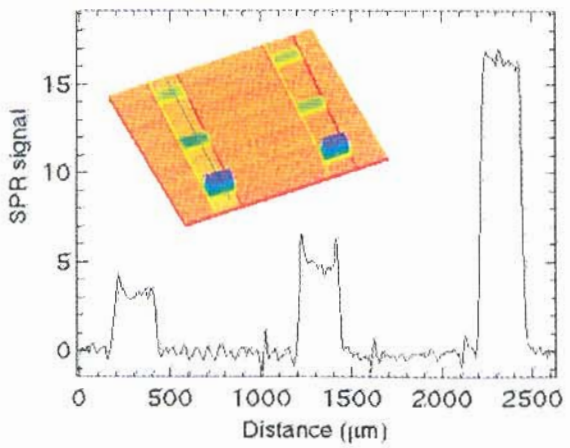

Figure 5.12 An SPR difference image showing adsorption of GUS gene ssRNA onto DNA probes. Each channel was 300 μm wide, 35 μm deep, and 1.2 μm long with 900 μm spacing between channels. Reprinted with permission from *Analytical Chemistry*, **73** 5525–5531. Copyright 2001 American Chemical Society.

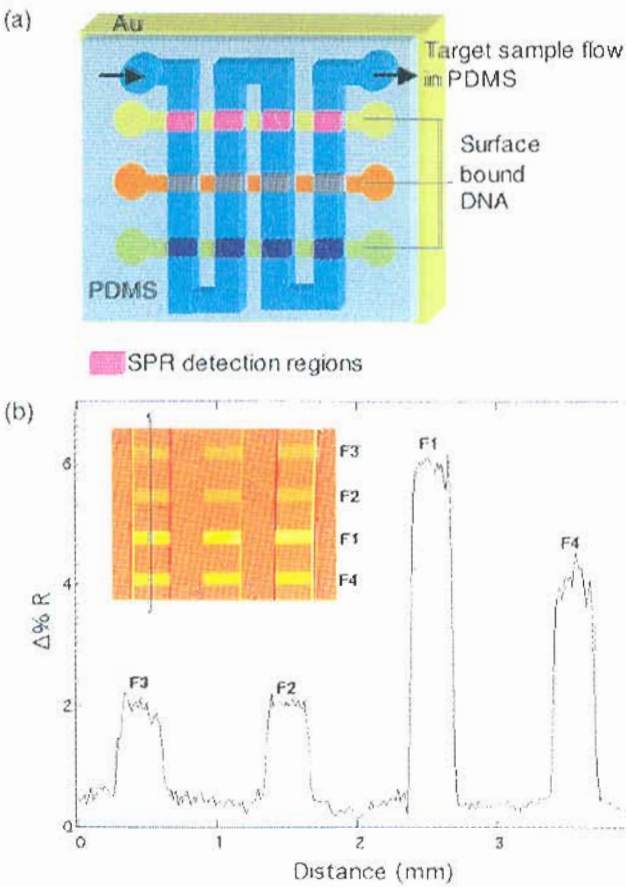

Figure 5.13 (a) A worm microchannel is used to deliver 5 μl aliquots of antibody solution to the peptide linear array. This microfluidic configuration is suitable for the delivery of a small volume of a single analyte to the array with a detection area equivalent to a configuration using a large volume flow cell. The worm channel was 500 μm wide, 35 μm deep, and 12 mm long with 500 μm spacing between channels.
(b) SPR difference image showing the adsorption of 100 nM anti-FLAG to a peptide array composed of four epitopes, differing by a single amino acid, based on the FLAG peptide sequence. The line profile reveals that the greatest adsorption occurs at elements containing the original sequence, F1. Diminished adsorption is observed at sequences, F3 and F4, containing alanine substitutions for essential residues of the binding motif. Peptide probe sequences can be found in the literature. Reprinted with permission from *Analytical Chemistry*, **74**, 5161–5168. Copyright 2002 American Chemical Society.

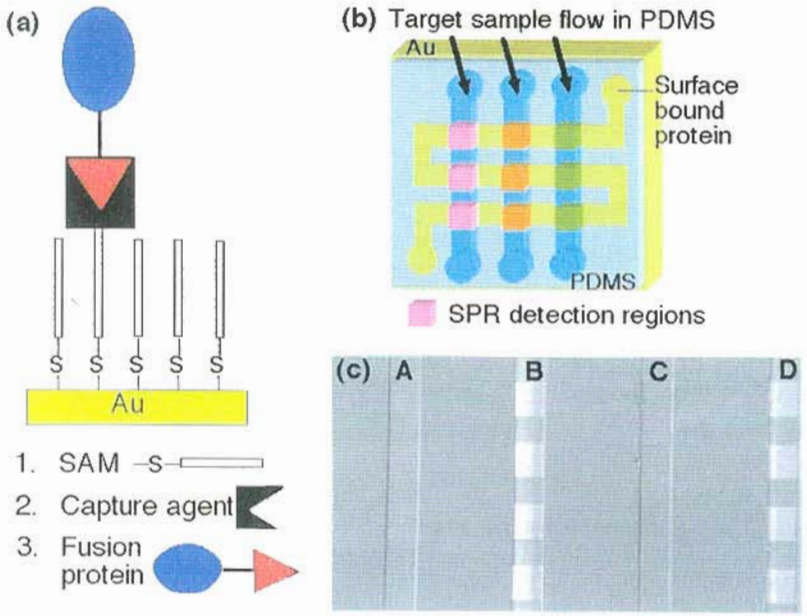

Figure 5.15 (a) Schematic representation of a general approach for the creation of an oriented fusion protein array on gold surfaces. (b) The NTA capture agent was immobilized through a worm microchannel. Next, a parallel set of PDMS channels was used to simultaneously deliver multiple histidine-tagged analytes to the NTA elements. (c) An example of an SPR difference image showing the immobilization of histidine-tagged ubiquitin **B** and polyhistidine D to NTA-modified monolayers in the presence of nickel ions. In the absence of nickel ions there is little non-specific adsorption of his-tagged ubiquitin **A** or polyhistidine **C** to the NTA surface, suggesting that a specific chelation interaction is occurring.